

Intranasal administration of mitochondria improves spatial memory in olfactory bulbectomized mice

Natalia V Bobkova¹, Daria Y Zhdanova¹, Natalia V Belosludtseva² , Nikita V Penkov¹ and Galina D Mironova² 

¹Institute of Cell Biophysics of the Russian Academy of Sciences-Federal Research Center, Pushchino Scientific Center for Biological Research of the Russian Academy of Sciences, 142290 Pushchino, Moscow Region, Russia; ²Institute of Theoretical and Experimental Biophysics of the Russian Academy of Sciences, 142290 Pushchino, Moscow Region, Russia

Corresponding authors: Galina D Mironova. Email: mironova@mail.ru; Natalia V Bobkova. Email: nbobkova@mail.ru

Impact statement

Mitochondrial dysfunction has been implicated in the pathogenesis of a number of neurodegenerative disorders, including Alzheimer's disease. The administration of functionally active mitochondria may attenuate cognitive impairments and recover the brain function. Olfactory bulbectomized mice, an animal model of depression with the symptoms of sporadic Alzheimer's disease, showed mitochondrial damage in the brain and the loss of spatial memory tested in the Morris water maze. Our findings demonstrate that the intranasal microinjections of mitochondria lead to the improvement of spatial memory in olfactory bulbectomized mice. The labeled mitochondria, when injected intranasally to recipient animals, are delivered dose-dependently to the neocortex and hippocampus, the brain regions responsible for learning and memory and most affected in Alzheimer's disease. The colocalization of allogeneic mitochondria with GFAP- and NeuN-positive cells in hippocampal cell culture was found. The results suggest that intranasal administration of mitochondria might serve as a new therapeutic strategy for neurodegenerative disorders.

Abstract

Here, we found that functionally active mitochondria isolated from the brain of NMRI donor mice and administrated intranasally to recipient mice penetrated the brain structures in a dose-dependent manner. The injected mitochondria labeled with the MitoTracker Red localized in different brain regions, including the neocortex and hippocampus, which are responsible for memory and affected by degeneration in patients with Alzheimer's disease. In behavioral experiments, intranasal microinjections of brain mitochondria of native NMRI mice improved spatial memory in the olfactory bulbectomized (OBX) mice with Alzheimer's type degeneration. Control OBX mice demonstrated loss of spatial memory tested in the Morris water maze. Immunocytochemical analysis revealed that allogeneic mitochondria colocalized with the markers of astrocytes and neurons in hippocampal cell culture. The results suggest that a non-invasive route intranasal administration of mitochondria may be a promising approach to the treatment of neurodegenerative diseases characterized, like Alzheimer's disease, by mitochondrial dysfunction.

Keywords: Mitochondrial therapy, intranasal microinjections, spatial memory, olfactory bulbectomized mice, neurodegenerative diseases, mitochondrial dysfunction

Experimental Biology and Medicine 2022; 247: 416–425. DOI: 10.1177/15353702211056866

Introduction

At present, “mitochondrial medicine” is an intense field of research, where dysfunctional mitochondria are a promising target of experimental therapeutic interventions for the prevention and treatment a number of pathologies,

including neurodegenerative diseases. As is known, mitochondria play a crucial role in the production of ATP, the metabolism of fatty and amino acids, and the regulation of ion homeostasis and other processes necessary for the normal functioning and survival of the cell.

A decline in the functional activity and quality of mitochondria is associated with the aging process¹ and a large number of severe cellular pathology.^{2–5} Alzheimer's disease (AD) and Parkinson's disease are distinguished examples of neurodegenerative diseases characterized by mitochondrial dysfunction.^{6–8} Functional and ultrastructural damage to mitochondria is an early and prominent feature of the AD⁹ and is associated with reduced cytochrome c oxidase (COX) activity¹⁰ and increased production of H₂O₂ and protein carbonyls, which are induced by A β transport into mitochondria⁴ and precede A β plaque formation.¹¹ The above-mentioned impairments were identified in the mice models of family and sporadic AD.^{4,12}

In *in vivo* experiments, novel therapeutic approaches to neurodegenerative diseases by the delivery of mitochondria to the brain were developed. These approaches include the injection of active mitochondria directly into the target structure, intracerebroventricular microinjections, intravenous administration,^{6,13} and the introduction of mitochondria-enriched cells.^{14,15} However, these invasive methods can have negative effects, such as thrombus formation and the risk of death. The use of mesenchymal stromal cells as sources of mitochondria through their local administration is traumatic and does not completely exclude the possibility of their malignant transformation.

Earlier, we have shown that in olfactory bulbectomized (OBX) mice, an animal model of depression with the main symptoms of sporadic AD,^{16,17} the level of amyloid- β peptide 1-40 (A β 1-40) is significantly higher not only in the tissues of the neocortex and hippocampus but also in mitochondria isolated from these regions of the brain.^{4,12} Intramitochondrial accumulation of soluble A β 1-40 is accompanied by the decline in the mitochondrial membrane potential, reduced activity of COX (respiratory chain complex IV), and increased level of lipid peroxidation products, indicating the development of oxidative stress. Behavioral tests showed that OBX mice displayed the loss of spatial memory. We suggested that mitochondrial dysfunction in the neurons of the OBX mouse brain might be an appropriate target for therapies by transplantation of a pool of functionally active mitochondria from neuronal tissue of native mice. To promote memory recovery in OBX mice, it is advisable to use a non-invasive route, namely, intranasal administration of functional mitochondria.

In the present work, we have examined whether intranasal administration of functionally active mitochondria affects the spatial memory impairment in OBX mice. The possibility of delivering mitochondria into the brain regions responsible for memory, namely the neocortex and hippocampus, as well as possible co-localization of allogeneic mitochondria with the markers of astrocytes and neurons have also investigated.

Materials and methods

Animals

Outbred NMRI male mice weighting 30–35 g (the age of the animals was around five or six months, $n = 15$) and 20–25 g

(the age of the animals was around three months, $n = 10$) were housed in groups of two to three per cage in a climate-controlled room for two weeks before experimental procedures under standard conditions at the room temperature of 18–22°C, relative humidity 60–70%, and regular 12-h light-dark cycles. The animals received commercial pellets and water ad libitum. The study with laboratory animals was carried out in accordance with the European Convention for the Protection of Vertebrates used for experimental and other purposes (Strasbourg, 1986), the principles of the Helsinki Declaration (2000), and the "Regulations for Studies with Experimental Animals" (Decree of the Russian Ministry of Health of August 12, 1997, No. 755). All the experimental protocols were approved by the Ethics Committees of ICB RAS and ITEB RAS (Protocol No. 09 of 01.03.2019). All surgery was performed under sodium pentobarbital anesthesia, and all efforts were made to minimize suffering.

Isolation of mouse brain mitochondria

Mitochondria were isolated from the brain of NMRI mice weighting 20–25 g by the conventional technique of differential centrifugation with minor modifications.¹⁸ Two brains of mice were quickly (within 1 min) withdrawn from the cranium and placed in an ice-cold saline. The chopped tissue was homogenized in the ice-cold isolation medium #1 (0.225 M mannitol, 0.075 M sucrose, 10 mM HEPES, 0.5 mM K-EGTA, 0.3% BSA, pH 7.4) and subjected to centrifugation 2000 g for 5 min. The supernatant was collected and centrifuged again at a higher rate (12,000 g \times 10 min). The pellet was washed with the medium #2 containing 0.225 M mannitol, 0.075 M sucrose, and 10 mM Hepes (pH 7.4) and sedimented (12,000 g \times 10 min), after which mitochondria were resuspended in the ratio of 1 g of the brain tissue to 0.1 ml of the medium #2. The resulting mitochondrial suspension contained 35–40 mg protein per 1 ml. The concentration of the protein was determined by the Lowry method. The final mitochondrial suspensions were diluted in the medium #2 to concentrations of 0.3, 1.8, and 3.3 mg/ml, which corresponds to 2, 10, and 20 μ g of injected mitochondrial protein per 6 μ L of solution (volume of solution for two intranasal injections, 3 μ L in each nostril of the mouse), correspondingly.

Labeling of mouse brain mitochondria with MitoTracker Red CMXRos

After centrifugation at 12,000 g, the mitochondria were labeled with MitoTracker Red CMXRos (MTR, Invitrogen, cat# M7512) according to the manufacturer's protocol. Briefly, mitochondria were incubated with 1 μ M MTR and respiration substrates (5 mM potassium glutamate, 5 mM potassium malate, and 10 mM potassium succinate) for 10 min at 4°C, covered from light. Then, the solution was centrifuged at 12,000 g \times 10 min at 4°C. The mitochondrial pellet was resuspended in medium #2 and washed two times by centrifugation at 12,000 g for 10 min to remove the unbound fluorescent dye. The resulting suspension of stained mitochondria was diluted to concentrations of 0.3,

1.8, and 3.3 mg/ml in medium #2 and used for further visualization in *in vitro* and *in vivo* experiments using a Leica DM IL LED Fluo fluorescence microscope (Germany).

Visualization of MTR-stained mitochondria in vitro

Suspensions of MTR-labeled mitochondria (0.3, 1.8, and 3.3 mg/ml) in a volume of 1 μ l were applied to a sterile glass slide and analyzed using a Leica DM IL LED Fluo microscope (Germany) ($\times 40$, Ex/Em: 579/599 nm). In each of three separate experiments performed on separate days, each dosage was applied to three different glass slides, and two random non-overlapping fields of view in each slide were captured using a fluorescent microscope representing the region of interest. After capturing the region of interest, the image was thresholded above background fluorescence, and red fluorescent objects were photographed.

Determination of respiration and oxidative phosphorylation of brain mitochondria

To assess the integrity and functional activity of isolated mitochondria, whether labeled or not, the rates of mitochondrial oxygen consumption and oxidative phosphorylation were assayed using the Oxygraph-2k high-resolution respirometer (O2k, Oroboros Instruments, Austria). The reaction medium contained 100 mM KCl, 75 mM mannitol 25 mM sucrose 0.5 mM EGTA-K, 5 mM KH_2PO_4 , and 10 mM Hepes/KOH, pH 7.4. The concentrations of substrates and other reagents were as follows: 2.5 mM potassium malate, 2.5 mM potassium glutamate (or 5 mM potassium succinate plus 1 μ M rotenone), 0.2 mM ADP, and 50 μ M 2,4-dinitrophenol (DNP). The concentration of mitochondrial protein in an oxygen cell was 0.5 mg/mL. Estimated were the mitochondrial respiration in state 3 (exogenous substrates plus ADP), in state 4 (after ADP depletion), and uncoupled state 3 U_{DNP} in the presence of the uncoupler DNP. The ADP/O coefficient (the amount of ADP per O consumed during state 3 respiration, μ M ADP/nmol O) and the time of ADP phosphorylation (T_{phos} , s) were determined as described previously.¹⁸

Intranasal microinjections of MTR-labeled mitochondria in vivo

NMRI mice were injected with 2 to 20 μ g of freshly isolated mitochondria in a volume of 3 μ l into each nostril (total volume 6 μ l/mouse). Four experimental groups of mice were formed: (1) control animals receiving a solution with non-labeled mitochondria at a dose of 10 μ g; (2) animals injected with a solution of MTR-stained mitochondria at a dose 2 μ g; (3) animals injected with a solution of MTR-stained mitochondria at a dose 10 μ g; and (4) animals that received a solution of MTR-stained mitochondria at a dose of 20 μ g. All mice were anesthetized with sodium pentobarbital (60 mg/kg i.p.), perfused transcardially with 20 mL of saline, and decapitated under sterile conditions 48 h after intranasal injections. The brain was quickly removed and placed on an ice-cold glass slide. The following brain structures have been identified, isolated, and briefly placed at

–20°C: the hippocampus, neocortex, and olfactory bulbs. On the same day, a homogenate from each structure in physiological saline was prepared and placed on a previously cleaned glass slide in the form of a cytological smear for microscopic examination using a Leica DM IL LED Fluo fluorescent microscope (Germany). The presence of mitochondria stained with the MTR fluorescent dye was assessed in at least 10 fields of view per smear, and photographs were taken.

Bilateral olfactory bulbectomy

The effect of intranasal administration of functionally active mitochondria was studied using olfactory bulbectomized (OBX) mice with Alzheimer's type degeneration accompanied by memory loss.¹⁶ Male six-month-old NMRI mice ($n = 15$) were used in experiments. During a sterile operation for the removal of the olfactory bulbs (olfactory bulbectomy), mice were anaesthetized with Nembutal (40 mg/kg, i.p.) and 0.5% Novocaine for local anesthesia of the scalp. Both olfactory bulbs were aspirated through a burr hole with the coordinates L0; AP-2; H3. Sham-operated (SO) mice underwent the same procedure, except for the olfactory bulb ablation.

Two weeks after bulbectomy mice were injected three times intranasally with 6 μ l solution of 3.3 μ g/ μ l mitochondria isolated from the brain of control (untreated) NMRI mice. Three intranasal injections of mitochondria were given over three weeks: two weeks before and one during the training period. The same volume of PBS was given to SO and OBX mice used as controls.

Memory tests

Memory tests were started two weeks after beginning of the mitochondrial administration. Learning of a navigational reflex in the Morris water maze was performed as described earlier¹⁶ and used as a training model. In experiments, a circular pool 80 cm in diameter filled with water (23°C) to a depth of 30 cm was conventionally divided into four equal sectors one of which, the target sector, contained a hidden save platform at a depth of 0.5 cm. The platform was 5 cm in diameter and invisible to swimming animals in milk-whitened water. The NMRI mice from all experimental groups were given four pre-training trials to determine their latent period of finding an exposed (visible) platform in order to verify that they did not have motor or visual impairments that could affect the results of memory tests. A five-day training period included four training trials daily with recording the latent periods of finding the invisible platform. It was followed by spatial memory probes implying the absence of the save platform for 1 min. The memory was considered to be good if the mice stayed in the target sector reliably longer or visited it more frequently than any indifferent sector. The state of spatial memory is assessed according to two criteria: the time spent in the sectors of the pool and the number of visits to them, expressed in %.

Cell culture

Primary culture of hippocampal cells from the brain of newborn NMRI mice (1–2 days after the birth) was cultivated according to the conventional technique. The suspension of isolated hippocampal cells was added to the wells of a six-well plate, the bottom of which was pretreated with poly-D-lysine (Gibco, USA). The mouse hippocampus cells were cultivated in Neurobasal medium (Gibco, USA) supplemented with B27 (Gibco, USA) and 1% Penicillin-Streptomycin-Glutamine (Gibco, USA) at 37°C in 5% CO₂ atmosphere. On the fourth day of cultivation, the hippocampal cell cultures at a density of about 120,000 cells per well were incubated with MTR-labeled mitochondria (20 µg) for 3 h, and then used for immunocytochemical analysis.

Immunocytochemical staining

Cell cultures were fixed with 4% paraformaldehyde for 10 min, and the cell membrane permeability was increased with 0.1% Triton X-100. Nonspecific binding sites were blocked with 5% BSA for 1 h at room temperature. Thereafter, the cell cultures were incubated with anti-NeuN mouse monoclonal antibody (Sigma-Aldrich #MAB377, 1:100) or anti-GFAP rabbit polyclonal antibody (Abcam #ab7260, 1:200) for 12 h at 4° C, after which the cell cultures were stained with DyLight 488-conjugated secondary antibody (Abcam #ab96871) or Alexa Fluor 488-conjugated secondary antibody (Abcam #ab150077), respectively. After each procedure, the cell cultures were washed with PBS three times for 5 min. The samples were inspected under a confocal microscope Leica TSC SP5 (Germany) with a HCX PL APO CS 10.0 × 0.40 UV objective. Fluorescence was excited by a laser with $\lambda = 488$ nm and registered in the spectral range channels of 403–459 nm and 599–695 nm. At least 10 fields of view were analyzed for each coverslip. Background staining was checked on samples of control cell cultures by removing the primary antibody. These samples displayed no immunogenic staining. For colocalization assay, the images were further

processed with the ImageJ program with Bio-Formats plugins (designed at the National Institutes of Health, Bethesda, MD, USA) as described in.¹⁹ The 8-bit images were converted into binary masks (Figure 6(a), (b), (e), and (f)). The merged images (Figure 6(c) and (g)) were obtained with the standard ImageJ operator “AND” from “Image Calculator.”

Statistical analysis

The data were analyzed using GraphPad Prism 8 (Graphpad Software, Inc., La Jolla, CA) and presented as means ± SEM. Statistical analysis of the results of probe tests was carried out with one-way ANOVA using group and sector of the maze as sources of variations. The preference for the target sector in comparison with each indifferent sector was assessed by *post hoc* analysis using Tukey criteria. Statistical significance was set to $p < 0.05$.

Results

Functional assessment of isolated mouse brain mitochondria in vitro

Mitochondria were isolated from the brain of three-month-old NMRI mice in 60 min in the presence of EGTA and BSA to avoid calcium and fatty acid-induced mitochondrial damage. To confirm the integrity and function of our mitochondrial preparations, the parameters of the efficiency of oxidative phosphorylation were measured. It was shown that isolated mitochondria demonstrate high values of ADP-stimulated respiration rate (state 3), ADP/O index, and a short time of ADP phosphorylation when using substrates of both complex I (NADH:ubiquinone oxidoreductase) and complex II (succinate dehydrogenase) of the respiratory chain, which indicates a high functional activity of the organelles (Figure 1; Table 1). When the mitochondria were stained with the mitochondrion-specific fluorescent probe MitoTracker Red CMXRos (MTR), they showed obvious red fluorescence. The fluorescence intensity depended on the used concentration of MTR-labeled

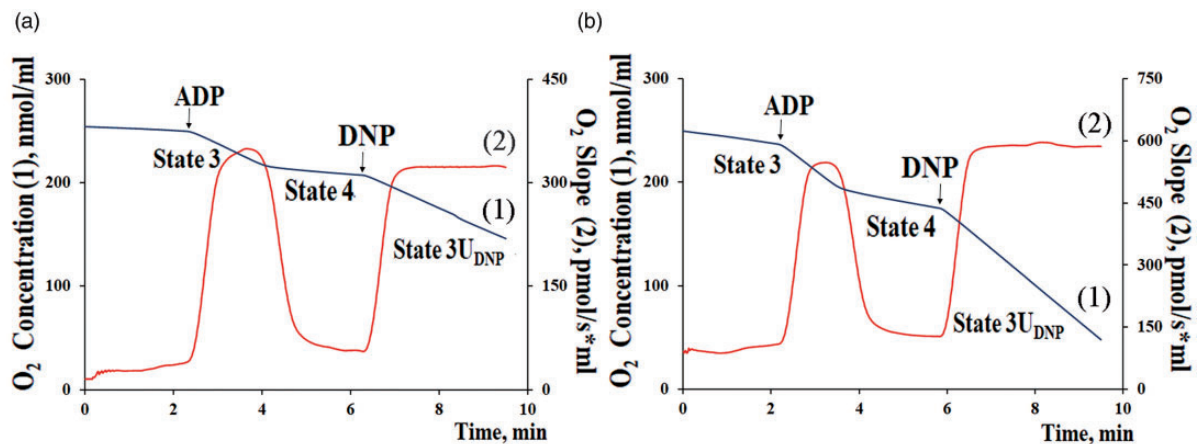


Figure 1. Typical curves of oxygen consumption by mouse brain mitochondria with the substrates of complex I (2.5 mM potassium malate + 2.5 mM glutamate) (a) or complex II (5 mM potassium succinate) (b). Final volume: 2 ml, temperature 25 °C, 0.5 mg/ml of mitochondrial protein. The medium contained 100 mM KCl, 75 mM mannitol 25 mM sucrose 0.5 mM EGTA-K, 5 mM KH₂PO₄, and 10 mM HEPES/KOH, pH 7.4. Additions: 0.2 mM ADP and 50 µM 2,4-dinitrophenol (DNP). (A color version of this figure is available in the online journal.)

Table 1. Rates of respiration and parameters of oxidative phosphorylation of brain mitochondria of NMRI mice in the presence of substrates of complex I (potassium malate + potassium glutamate) and complex II (potassium succinate) of the respiratory chain.

Substrates	Respiration rates, nmol O ₂ /min-mg				T _{Phosp.} (s)
	State 3	State 4	State 3U _{DNP}	ADP/O	
Malate + glutamate	42.32 ± 2.24	6.86 ± 0.80	39.65 ± 2.10	2.95 ± 0.05	54.32 ± 3.10
succinate	64.57 ± 3.26	15.10 ± 1.92	67.08 ± 8.12	1.92 ± 0.05	58.74 ± 3.13

The incubation medium contained 100 mM KCl, 75 mM mannitol, 25 mM sucrose, 5 mM KH₂PO₄, 0.5 mM EGTA, 10 mM Hepes/KOH (pH 7.4). Additions: 2.5 mM potassium malate + 2.5 mM potassium glutamate or 5 mM potassium succinate + 1 μM rotenone, 200 μM ADP, and 50 μM 2,4-dinitrophenol (DNP). The concentration of mitochondrial protein in the cuvette was 0.5 mg/ml. Mitochondrial respiration rates, nmol O₂/min-mg; ADP/O, μM/nmol O; T_{phos}, s. Data are presented as the means ± S.E.M. (n = 3).

mitochondria. Figure 2 shows the fluorescence signals from suspensions of MTR-labeled mitochondria at concentrations of 0.3, 1.8, and 3.3 mg/ml. At the same time, there is no signal from the control (native) mitochondria. These results suggested that isolated mitochondria remain coupled and functionally active and can be used for further investigations.

Intranasally administrated mitochondria are detected in the hippocampus, neocortex, and olfactory bulbs of recipient mice

The first series of experiments is devoted to elucidating the possibility of delivering mitochondria into the brain after their intranasal administration. Freshly prepared suspensions of MTR-labeled mitochondria at concentrations of 0.3, 1.8, and 3.3 mg/ml were injected intranasally to six-month-old male NMRI mice once in a volume of 6 μl per animal (3 μl in each nostril), which corresponds to 2, 10, and 20 μg of injected mitochondrial protein per animal. Control animals received intranasal injections of unlabeled mitochondria (10 μg) in the same volume. All animals were under observation for two days. No toxicity of intranasal administration of isolated mitochondria to mice was revealed. The brain structures were isolated 48 h after administration and visualized using a fluorescent microscope.

Figures 3 and 4 present representative micrographs of cytological smears of the hippocampus and neocortex of NMRI mice. For each smear, images in the red spectral region and in transmitted light are presented. As can be seen, the fluorescence signals are observed in tissue samples of the hippocampus and, to a lesser extent, in the neocortex of mice with intranasally injected suspensions of MTR-labeled mitochondria at doses of 10 and 20 μg per mice. It should be noted that MTR-labeled mitochondria were also found in the region of the olfactory bulbs (Supplementary materials; Figure S1). We detected no fluorescence signal in the smears of brain areas in mice with intranasal administration of PBS or unstained mitochondria. The positive signal is not due to autofluorescence because of lack of co-localization with signal in the 488 channel.

Our results demonstrate that nasally administrated mitochondria are dose-dependently transplanted into the hippocampus and neocortex, that is, in the main areas of the brain involved in learning and memory.

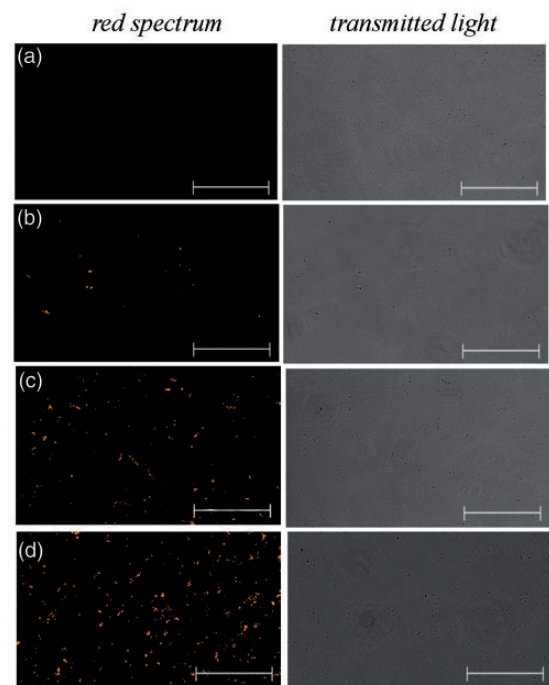


Figure 2. Micrographs of suspensions of unstained mitochondria at a concentration of 1.8 mg/ml (negative control) (a) and MTR-stained mitochondria at concentrations of 0.3 mg/ml (b), 1.8 mg/ml (c), and 3.3 mg/ml (d). Representative images in the red spectral region are presented (n = 3). The scale bar: 25 μm. (A color version of this figure is available in the online journal.)

The effect of intranasal administration of brain mitochondria on the spatial memory of OBX mice

To investigate whether intranasal administration of mitochondria could ameliorate the spatial memory impairment that characterize AD pathogenesis, we performed behavioral analyses using OBX mouse model. A schematic illustration of the experimental design is shown in Figure 5(a). The effect of three-time intranasal injections of brain mitochondria of control NMRI mice (at a dose of 20 μg per one microinjection) on the state of spatial memory in NMRI mice with surgically removed olfactory bulbs was analyzed (for one-way ANOVA-based data, see Table 2; the Post hoc analysis of staying times and visit frequencies for four sectors of the Morris water maze is shown in Figure 5(b)).

OBX mice were treated either with mitochondria or PBS. One can see that mitochondria-untreated OBX + PBS mice showed a considerable impairment of spatial memory, while OBX mice treated with mitochondria notably

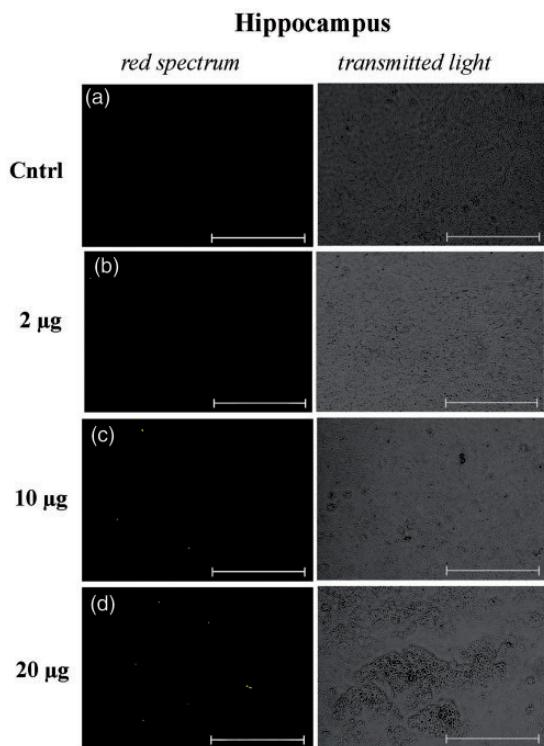


Figure 3. Micrographs of cytological smears of the hippocampus of control NMRI mice, which were injected with solutions with unstained mitochondria at a dose of 10 µg per mouse (negative control) (a) and MTR-stained mitochondria at doses of 2 µg (b), 10 µg (c), and 20 µg (d) per mouse. Representative images in the red spectral region (left panel) and in the transmitted light (right panel) are presented ($n = 3$). The scale bar: 50 µm. (A color version of this figure is available in the online journal.)

preserved their memory and distinguished the sector that during training trials contained the invisible save platform.

Importantly, the positive effects of mitochondrial administration were observed on two indicators of spatial memory, the duration of staying in the target (third) sector and the frequency of visits to it. In sham operated (SO+PBS), OBX+PBS, and mitochondria-treated OBX (OBX+Mito) mice, the time of staying in the target sector was $22 \pm 1.5 > 11.4 \pm 0.8 < 19.3 \pm 1.4$ s, respectively, and the percentage of visiting in the target sector (*vs.* the total number of visits to all sectors) was $35.3 \pm 2.2 > 21.7 \pm 1.3 < 30.7 \pm 1.6\%$, respectively.

Identification of MTR-labeled allogenic mitochondria in astrocytes and neurons of primary hippocampal cell culture of NMRI mice

To determine the types of mouse brain cells into which mitochondria can be transferred, the MPR-labeled allogenic mitochondria were incubated with the primary hippocampal cell culture of NMRI mice, and their localization was identified by immunofluorescence analysis using antibodies against glial fibrillary acidic protein (GFAP) and neuronal nuclear protein (NeuN) as markers for reactive astrocytes and neurons, correspondingly. As shown in Figure 6(a) to (d), the labeled mitochondria demonstrated an obvious co-localization with the GFAP-positive cells. At the same time, the co-localization of the mitochondria with

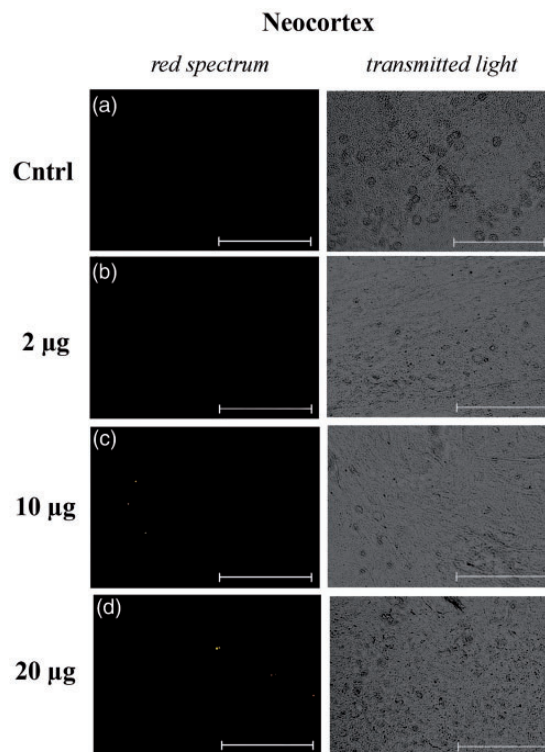


Figure 4. Micrographs of cytological smears of the neocortex of control NMRI mice, which were injected with solutions with unstained mitochondria at a dose of 10 µg per mouse (negative control) (a) and MTR-stained mitochondria at doses of 2 µg (b), 10 µg (c) and 20 µg (d) per mouse. Representative images in the red spectral region (left panel) and in transmitted light (right panel) are presented ($n = 3$). The scale bar: 50 µm. (A color version of this figure is available in the online journal.)

NeuN-positive cells demonstrated a rare pattern (Figure 6 (e) to (h)). The results suggest that allogenic mitochondria can be transferred both to astrocytes and, albeit to a much lesser extent, to neurons.

Discussion

In this work, we showed that mouse brain mitochondria, when injected to recipient animals via a non-invasive intranasal route, were delivered to the brain structures in a dose-dependent manner. Labeled mitochondria were detected in the neocortex and hippocampus, the brain regions responsible for learning and memory and most affected in Alzheimer's disease. The intranasal microinjections of brain mitochondria isolated from intact (healthy) NMRI mice at a dose of 20 µg/animal three times over three weeks improved the characteristics of the spatial memory of OBX mice with Alzheimer's type degeneration compared to those of untreated control animals.

The results of memory tests indicated that intranasal administration of mitochondria prevents the impairment of spatial memory of OBX animals. One can propose that the intranasal route provides the introduction of mitochondria into the brain by direct delivery of mitochondria from the nasal cavity to the brain, bypassing the blood-brain barrier, which ensures therapeutic action and minimal invasiveness due to the absence of peripheral side effects.^{20,21} It is known that along with the olfactory

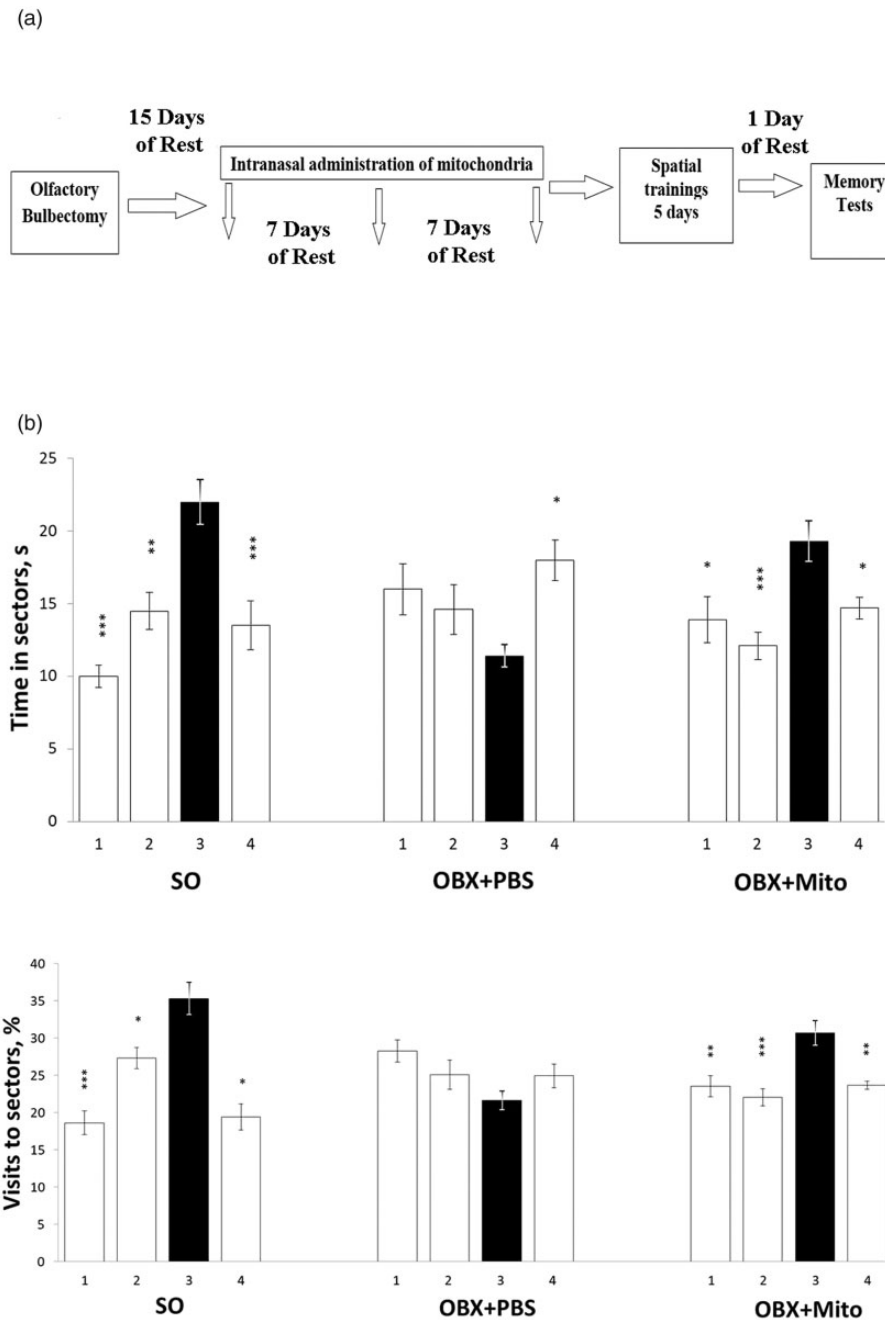


Figure 5. Scheme of the experiment (a) and the effect of intranasal administration of brain mitochondria (20 $\mu\text{g}/\text{mouse}$) on the indicators of spatial memory of sham-operated (SO), olfactory bulbectomized (OBX+PBS), and mitochondria-treated OBX (OBX+Mito) mice (b). The shaded bars correspond to the parameters in the target third sector. 1–4 – the sector numbers of the Morris water maze. Statistically significant differences between the groups were identified by the Tukey's HSD analysis: * $p < 0.05$; ** $p < 0.01$; *** $p < 0.001$ ($n = 5$).

nerves, there are several other pathways of penetration of mitochondria and drugs into the brain after their intranasal administration, in particular, the mandibular and maxillary segment of the trigeminal nerve, specialized myelinating glia that can form cerebrospinal fluid-filled cavities, which are thought to be involved in extracellular trafficking. Some studies demonstrated that the delivery of intranasally administered agents occurs within a short time period (5–30 min), suggesting the important roles of extracellular transport and bulk flow mechanisms.^{22–26}

Currently, intranasal microinjections are used for the transplantation of stem cells.²⁷

It is well established that in the central nervous system, mitochondria can be horizontally transferred between cells. In particular, neurons were found to release damaged mitochondria into astrocytes for their disposal or recycling under normal conditions.²⁸ In its turn, during cerebral infarction, astrocytes demonstrated the ability to transmit functionally active mitochondria to neurons, which may maintain their functions.²⁹ Moreover, the neuroprotective

Table 2. Values of the sector distinguishing factor for different groups of mice in memory tests in the Morris water maze.

Group	Staying in the Morris maze sectors Time, s		Visits to the Morris maze sectors Frequency, %	
	F	P value	F	P value
SO + PBS (n = 12)	F(3,44) = 13,6	<0.0001***	F(3,44) = 20,18469	<2,23628E-08***
OBX + PBS (n = 10)	F(3,36) = 3.62762	<0.021923*	F(3,36) = 2,90881	<0,047716189*
OBX + Mito (n = 10)	F(3,36) = 6.39657	<0,001379**	F(3,36) = 9,67788	<8,02356E-05***

* $p < 0.05$; ** $p < 0.01$; *** $p < 0.001$ (n = 5).

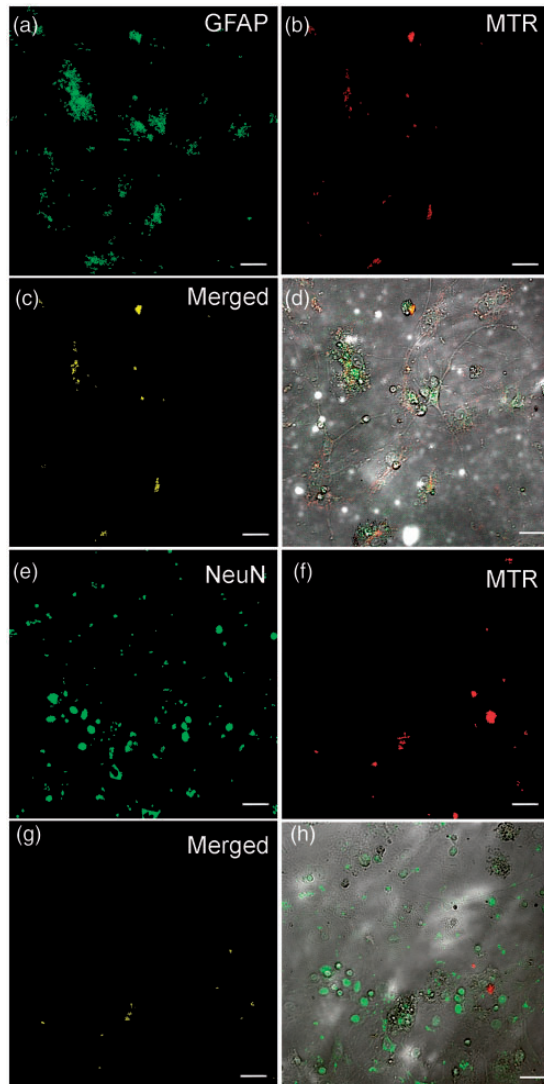


Figure 6. Identification of MTR-labeled allogenic mitochondria in astrocytes (a–d) and neurons (e–h) of NMRI mouse hippocampal cell culture. Co-staining GFAP (marker for astrocytes, green) or NeuN (marker for neurons, green) with MitoTracker Red (MTR)-labeled mitochondria (red). (c and g) The merged images of binary masks of AF488 anti-GFAP (or DL488 anti-NeuN) and MTR channels. (d and h) The merged images of transmitted light, AF488 anti-GFAP (or DL488 anti-NeuN), and MTR channels. The scale bar: 25 μ m. (A color version of this figure is available in the online journal.)

effect of transplantation of endothelial progenitor cells was observed to be mediated through the transfer of active mitochondria released from the progenitors.^{30,31} Recent data showed that transferring exogenous mitochondria to the injured hippocampal neurons in primary cell cultures

not only significantly increases neurite regrowth but also restores their membrane potential.³² The beneficial effects of mitochondrial transplantation on ischemic brain injury³³ and ischemia/reperfusion-induced myocardial injuries³⁴ have been proven in animal models. It has also been found that blood contains circulating cell-free respiratory competent mitochondria,³⁵ but the possible functions and mechanism of extrusion of these extracellular mitochondria is still unclear.

Numerous *in vivo* and *in vitro* studies reported that intercellular mitochondrial transfer can occur under physiological and pathological conditions via tunneling nanotubes, extracellular vesicles, cellular fusion, and gap junctions.³⁶ At the same time, the molecular mechanism of mitochondrial transfer needs to be further investigated. Using fluorescent labeling of primary hippocampal cell culture of NMRI mice, we found co-localization of allogenic mitochondria with astrocytes, and in rare cases, with neurons as well. A rare pattern of colocalization of allogenic mitochondria with neurons may be associated with insufficient molecular interactions between cultured cells. It should be noted that the transfer of extracellular mitochondria from astrocytes to neurons is mediated by a calcium-dependent mechanism involving CD38 and cyclic ADP ribose signaling.²⁹ Some studies also demonstrated only a negligible localization of the injected mitochondria into the cells of the spinal cord and myocardium.^{37,38}

Our findings provide evidence of the therapeutic efficacy of intranasal administration of functionally active mitochondria in the prevention of memory loss in animals with the neurodegenerative process of the Alzheimer's type. The restoration of cognitive function may be associated with the reversion of underlying mitochondrial dysfunction of astrocytes and neurons in the hippocampus. It should be mentioned that similar results were obtained recently on the mouse model of cisplatin-induced cognitive deficits.²¹ The authors showed that the intranasally injected mitochondria accessed the rostral migratory stream and other brain regions, including the hippocampus, where they colocalized, as in our experiments, with the GFAP-positive cells.²¹

The results obtained suggest that mitochondrial transplantation by intranasal administration might serve as a new therapeutic strategy for AD and other neurodegenerative diseases characterized by mitochondrial dysfunction. These data were included in the patent "Targeted non-invasive transplantation of functionally active mitochondria into the brain for the treatment of neurodegenerative disease characterized by mitochondrial dysfunction"

(Patent Application Number: RU2744453 dated September 2, 2019).

AUTHORS' CONTRIBUTIONS

GDM proposed the project and wrote the manuscript; NV Bobkova supervised the study, designed experiments, and wrote the manuscript; DYZ and NVB performed main experiments and analyzed results; NVP performed colocalization assay. All authors read and approved the final manuscript.

ACKNOWLEDGMENTS

We are sincerely grateful to Alexander Nadeev for help with language editing.

DECLARATION OF CONFLICTING INTERESTS


The author(s) declared no potential conflicts of interest with respect to the research, authorship, and/or publication of this article.

FUNDING

The author(s) disclosed receipt of the following financial support for the research, authorship, and/or publication of this article: This work was supported by the Russian Science Foundation (Grant number 18-15-00392, <https://rscf.ru/project/18-15-00392/>; visualization of MTR-stained mitochondria *in vitro*, intranasal administration of mitochondria, behavioral experiments *in vivo*, investigation of colocalisation of MTR-stained mitochondria with astrocytes and neurons in primary cell culture, Table 2 and Figures 2 to 6) and the Russian Foundation for Basic Research (Grant number 20-015-00029A, procedure for isolation, staining, functional assessment of mitochondria, Table 1 and Figure 1).

ORCID IDS

Natalia V Belosludtseva  <https://orcid.org/0000-0001-5707-6557>

Galina D Mironova  <https://orcid.org/0000-0001-7432-0902>

SUPPLEMENTAL MATERIAL

Supplemental material for this article is available online.

REFERENCES

- Chiavellini P, Canatelli-Mallat M, Lehmann M, Gallardo MD, Herenu CB, Cordeiro JL, Clement J, Goya RG. Aging and rejuvenation – a modular epigenome model. *Aging (Albany NY)* 2021;**13**:4734–46
- Nunnari J, Suomalainen A. Mitochondria: in sickness and in health. *Cell* 2012;**148**:1145–59
- Mironova GD, Pavlik LL, Kirova YI, Belosludtseva NV, Mosentsov AA, Khmil NV, Germanova EL, Lukyanova LD. Effect of hypoxia on mitochondrial enzymes and ultrastructure in the brain cortex of rats with different tolerance to oxygen shortage. *J Bioenerg Biomembr* 2019;**51**:329–40
- Avetisyan AV, Samokhin AN, Alexandrova IY, Zinovkin RA, Simonyan RA, Bobkova NV. Mitochondrial dysfunction in neocortex and hippocampus of olfactory bulbectomized mice, a model of Alzheimer's disease. *Biochemistry (Mosc)* 2016;**81**:615–23
- Belosludtsev KN, Belosludtseva NV, Dubinin MV. Diabetes mellitus, mitochondrial dysfunction and Ca²⁺-dependent permeability transition pore. *Int J Mol Sci* 2020;**21**:6559
- Shi X, Zhao M, Fu C, Fu A. Intravenous administration of mitochondria for treating experimental Parkinson's disease. *Mitochondrion* 2017;**34**:91–100
- Mosentsov AA, Rozova EV, Belosludtseva NV, Mankovskaya IN, Putiy YV, Karaban IN, Mikheeva IB, Mironova GD. Does the operation of mitochondrial ATP-dependent potassium channels affect the structural component of mitochondrial and endothelial dysfunctions in experimental parkinsonism? *Bull Exp Biol Med* 2021;**170**:431–5
- Compagnoni MG, Di Fonzo A, Corti S, Comi GP, Bresolin N, Masliah E. The role of mitochondria in neurodegenerative diseases: the lesson from Alzheimer's disease and Parkinson's disease. *Mol Neurobiol* 2020;**57**:2959–80
- Oliver DA, Reddy PH. Molecular basis of Alzheimer's disease: focus on mitochondria. *J Alzheimers Dis* 2019;**72**:S95–S116
- Schmitt K, Grimm A, Kazmierczak A, Strosznajder JB, Gotz J, Eckert A. Insights into mitochondrial dysfunction: aging, amyloid B, and tau – a deleterious trio. *Antioxid Redox Signal* 2012;**16**:1456–66
- Cha MY, Han SH, Son SM, Hong HS, Choi YJ, Byun J, Mook-Jung I. Mitochondria-specific accumulation of amyloid β induces mitochondrial dysfunction leading to apoptotic cell death. *PLoS One* 2012;**7**:e34929
- Avetisyan A, Balasanyants S, Simonyan R, Koroev D, Kamynina A, Zinovkina R, Bobkova N, Volpina O. Synthetic fragment (60–76) of rage improves brain mitochondria function in olfactory bulbectomized mice. *Neurochem Int* 2020;**140**:104799
- Nitzan K, Benhamron S, Valitsky M, Kesner EE, Lichtenstein M, Ben-Zvi A, Ella E, Segalstein Y, Saada A, Lorberboum-Galski H, Rosenmann H. Mitochondrial transfer ameliorates cognitive deficits, neuronal loss, and gliosis in Alzheimer's disease mice. *J Alzheimers Dis* 2019;**72**:587–604
- Hsu YC, Wu YT, Yu TH, Wei YH. Mitochondria in mesenchymal stem cell biology and cell therapy: from cellular differentiation to mitochondrial transfer. *Semin Cell Dev Biol* 2016;**52**:119–31
- Ma H, Jiang T, Tang W, Ma Z, Pu K, Xu F, Chang H, Zhao G, Gao W, Li Y, Wang Q. Transplantation of platelet-derived mitochondria alleviates cognitive impairment and mitochondrial dysfunction in Db/Db mice. *Clin Sci (Lond)* 2020;**134**:2161–75
- Bobkova NV, Lyabin DN, Medvinskaya NI, Samokhin AN, Nekrasov PV, Nesterova IV, Aleksandrova IY, Tarnarikova OG, Bobylev AG, Vikhlyantsev IM, Kukharsky MS, Ustyugov AA, Polyakov DN, Eliseeva IA, Kretov DA, Guryanov SG, Ovchinnikov LP. The Y-Box binding protein 1 suppresses Alzheimer's disease progression in two animal models. *PLoS ONE* 2015;**10**:e0138867
- Bobkova N, Vorobyov V, Medvinskaya N, Nesterova I, Tarnarikova O, Nekrasov P, Samokhin A, Deev A, Sengpiel F, Koroev D, Volpina O. Immunization against specific fragments of neurotrophin p75 receptor protects forebrain cholinergic neurons in the olfactory bulbectomized mice. *J Alzheimers Dis* 2016;**53**:289–301
- Venediktova NI, Gorbacheva OS, Belosludtseva NV, Fedotova IB, Surina NM, Poletaeva II, Kolomytkin OV, Mironova GD. Energetic, oxidative and ionic exchange in rat brain and liver mitochondria at experimental audiogenic epilepsy (Krushinsky-Molodkina model). *J Bioenerg Biomembr* 2017;**49**:149–58
- Berezhnov AV, Soutar MPM, Fedotova EI, Frolova MS, Plun-Favreau H, Zinchenko VP, Abramov AY. Intracellular pH modulates autophagy and mitophagy. *J Biol Chem* 2016;**291**:8701–8
- Ruigrok MJR, de Lange ECM. Emerging insights for translational pharmacokinetic and pharmacokinetic-pharmacodynamic studies: towards prediction of nose-to-brain transport in humans. *AAPS J* 2015;**17**:493–505
- Alexander JF, Sua AV, Arroyo LD, Ray PR, Wangzhou A, Heiβ-Lückemann L, Schedlowski M, Price TJ, Kavelaars A, Heijnen CJ. Nasal administration of mitochondria reverses chemotherapy-induced cognitive deficits. *Theranostics* 2021;**11**:3109–30
- Banks WA, Doring MJ, Niehoff ML. Brain uptake of the glucagon-like peptide-1 antagonist exendin(9–39) after intranasal administration. *J Pharmacol Exp Ther* 2004;**309**:469–75

23. Danielyan L, Beer-Hammer S, Stolzing A, Schäfer R, Siegel G, Fabian C, Kahle P, Biedermann T, Lourhmati A, Buadze M, Novakovic A, Proksch B, Gleiter CH, Frey WH, Schwab M. Intranasal delivery of bone marrow-derived mesenchymal stem cells, macrophages, and microglia to the brain in mouse models of Alzheimer's and Parkinson's disease. *Cell Transplant* 2014;**23**:S123-39
24. Danielyan L, Schafer R, von Ameln-Mayerhofer A, Buadze M, Geisler J, Klopfer T, Burkhardt U, Proksch B, Verleysdonk S, Ayturan M, Buniatian GH, Gleiter CH, Frey WH. Intranasal delivery of cells to the brain. *Eur J Cell Biol* 2009;**88**:315-24
25. Dhuria SV, Hanson LR, Frey WH. Intranasal delivery to the central nervous system: mechanisms and experimental considerations. *J Pharm Sci* 2010;**99**:1654-73
26. Battaglia L, Panciani PP, Muntoni E, Capucchio MT, Biasibetti E, Bonis PD, Mioletti S, Fontanella M, Swaminathan S. Lipid nanoparticles for intranasal administration: application to nose-to-brain delivery. *Expert Opin Drug Deliv* 2018;**15**:369-78
27. Li G, Bonamici N, Dey M, Lesniak MS, Balyasnikova IV. Intranasal delivery of stem cell-based therapies for the treatment of brain malignancies. *Expert Opin Drug Deliv* 2018;**15**:163-72
28. Davis CH, Kim KY, Bushong EA, Mills EA, Boassa D, Shih T, Kinebuchi M, Phan S, Zhou Y, Bihlmeyer NA, Nguyen JV, Jin Y, Ellisman MH, Marsh-Armstrong N. Transcellular degradation of axonal mitochondria. *Proc Natl Acad Sci U S A* 2014;**111**:9633-8
29. Hayakawa K, Esposito E, Wang X, Terasaki Y, Liu Y, Xing C, Ji X, Lo EH. Transfer of mitochondria from astrocytes to neurons after stroke. *Nature* 2016;**535**:551-5
30. Russo E, Nguyen H, Lippert T, Tuazon J, Borlongan CV, Napoli E. Mitochondrial targeting as a novel therapy for stroke. *Brain Circ* 2018;**4**:84-94
31. Garbuzova-Davis S, Haller E, Lin R, Borlongan CV. Intravenously transplanted human bone marrow endothelial progenitor cells engraft within brain capillaries, preserve mitochondrial morphology, and display pinocytotic activity toward blood-brain barrier repair in ischemic stroke rats. *Stem Cells* 2017;**35**:1246-58
32. Chien L, Liang MZ, Chang CY, Wang C, Chen L. Mitochondrial therapy promotes regeneration of injured hippocampal neurons. *Biochim Biophys Acta Mol Basis Dis* 2018;**1864**:3001-12
33. McCully JD, Cowan DB, Pacak CA, Toumpoulis IK, Dayalan H, Levitsky S. Injection of isolated mitochondria during early reperfusion for cardioprotection. *Am J Physiol Heart Circ Physiol* 2009;**296**:H94-H105
34. McCully JD, Cowan DB, Emani SM, Del Nido PJ. Mitochondrial transplantation: from animal models to clinical use in humans. *Mitochondrion* 2017;**34**:127-34
35. Al Amir Dache Z, Otandault A, Tanos R, Pastor B, Meddeb R, Sanchez C, Arena G, Lasorsa L, Bennett A, Grange T, Messaoudi SE, Mazard T, Prevostel C, Thierry AR. Blood contains circulating cell-free respiratory competent mitochondria. *FASEB J* 2020;**34**:3616-30
36. Torralba D, Baixauli F, Sanchez-Madrid F. Mitochondria know no boundaries: mechanisms and functions of intercellular mitochondrial transfer. *Front Cell Dev Biol* 2016;**4**:107
37. Gollihue JL, Patel SP, Eldahan KC, Cox DH, Donahue RR, Taylor BK, Sullivan PG, Rabchevsky AG. Effects of mitochondrial transplantation on bioenergetics, cellular incorporation, and functional recovery after spinal cord injury. *J Neurotrauma* 2018;**35**:1800-18
38. Li H, Wang C, He T, Zhao T, Chen YY, Shen YL, Zhang X, Wang LL. Mitochondrial transfer from bone marrow mesenchymal stem cells to motor neurons in spinal cord injury rats via gap junction. *Theranostics* 2019;**9**:2017-35

(Received May 25, 2021, Accepted October 12, 2021)